

# Development of a Microcontroller-Based, Photovoltaic Maximum Power Point Tracking Control System

Eftichios Koutroulis, Kostas Kalaitzakis, *Member, IEEE*, and Nicholas C. Voulgaris

**Abstract**—Maximum power point tracking (MPPT) is used in photovoltaic (PV) systems to maximize the photovoltaic array output power, irrespective of the temperature and irradiation conditions and of the load electrical characteristics. A new MPPT system has been developed, consisting of a Buck-type dc/dc converter, which is controlled by a microcontroller-based unit. The main difference between the method used in the proposed MPPT system and other techniques used in the past is that the PV array output power is used to directly control the dc/dc converter, thus reducing the complexity of the system. The resulting system has high-efficiency, lower-cost and can be easily modified to handle more energy sources (e.g., wind-generators). The experimental results show that the use of the proposed MPPT control increases the PV output power by as much as 15% compared to the case where the dc/dc converter duty cycle is set such that the PV array produces the maximum power at 1 kW/m<sup>2</sup> and 25 °C.

**Index Terms**—Battery charging, dc/dc converters, maximum power point tracking, microcontrollers, photovoltaic systems.

## I. INTRODUCTION

AS people are much concerned with the fossil fuel exhaustion and the environmental problems caused by the conventional power generation, renewable energy sources and among them photovoltaic panels and wind-generators are now widely used. Photovoltaic sources are used today in many applications such as battery charging, water pumping, home power supply, swimming-pool heating systems, satellite power systems etc. They have the advantage of being maintenance- and pollution-free but their installation cost is high and, in most applications, they require a power conditioner (dc/dc or dc/ac converter) for load interface. Since PV modules still have relatively low conversion efficiency, the overall system cost can be reduced using high efficiency power conditioners which, in addition, are designed to extract the maximum possible power from the PV module [maximum power point tracking (MPPT)].

A very common MPPT technique [1] is to compare the PV array voltage (or current) with a constant reference voltage (or current), which corresponds to the PV voltage (or current) at the maximum power point, under specific atmospheric conditions [Fig. 1(a)]. The resulting difference signal (error signal) is used to drive a power conditioner which interfaces the PV array to the load. Although the implementation of this method is simple,

the method itself is not very accurate, since it does not take into account the effects of temperature and irradiation variations.

In the PV current-controlled MPPT system [2] shown in Fig. 1(b), the PV array output current is compared with a reference current calculated using a microcontroller, which compares the PV output power before and after a change in the duty cycle of the dc/dc converter control signal. The PI controller regulates the PV output current to match the reference current.

The incremental conductance method proposed in [3] and [4] is based on the principle that at the maximum power point  $dP/dV = 0$  and, since  $P = VI$ , it yields

$$\frac{dV}{dI} = -\frac{I}{V} \quad (1)$$

where  $P$ ,  $V$ , and  $I$  are the PV array output power, voltage and current, respectively. This method is implemented [3] as shown in Fig. 1(c). A PI controller is used to regulate the PWM control signal of the dc/dc converter until the condition:  $(dI/dV) + (I/V) = 0$  is satisfied. This method has the disadvantage that the control circuit complexity results in a higher system cost.

Alternatively, as proposed in [5], the power slope  $dP/dV$  can be calculated digitally by sampling the PV array output current  $I$  and voltage  $V$  at consecutive time intervals  $(n-1)$  and  $(n)$  as follows:

$$\frac{dP}{dV}(n) = \frac{P(n) - P(n-1)}{V(n) - V(n-1)} \quad (2)$$

where

$$P(n) = V(n)I(n).$$

The power slope given in (2) can be applied to a PI controller driving a dc/dc converter until  $dP/dV = 0$ . Since this method requires a fast calculation of the power slope, its implementation is expensive.

For battery charging applications, where the dc/dc converter output voltage can be assumed almost constant, a feed-forward MPPT controller [6] may be applied, as shown in Fig. 1(d). The value of the battery charging current is used to directly control the duty cycle of the PWM control signal applied to the dc/dc converter. An output power increase results in both higher output current and higher PWM control signal duty cycle, until the maximum power is transferred to the load. This method has

Manuscript received April 27, 1999; revised September 25, 2000. Recommended by Associate Editor P. K. Jain.

The authors are with the Department of Electronic and Computer Engineering, Technical University of Crete, Chania GR-73100, Greece.

Publisher Item Identifier S 0885-8993(01)00979-6.

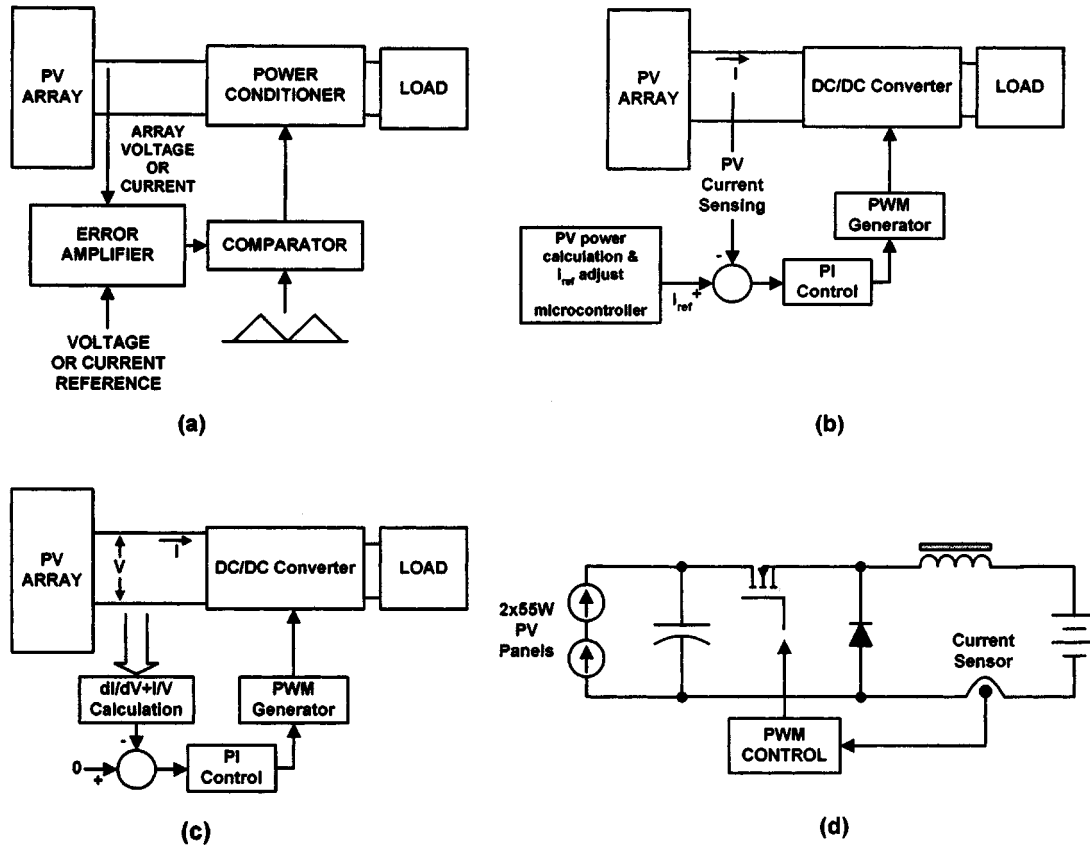


Fig. 1. Past proposed MPPT control systems. (a) MPPT control system with constant voltage or current reference. (b) MPPT control system with current reference. (c) MPPT system with the incremental conductance control method. (d) Feed-forward maximum power tracking control system.

the disadvantage that it can be used only in applications where the output voltage remains relatively constant.

In the method described in [7], the power converter is controlled using the PV array output power [Fig. 2(a)]. The MPPT control algorithm [Fig. 2(b)] is based on the calculation of the PV output power and of the power change by sampling voltage and current values. The power change is detected by comparing the present and previous voltage levels, in order to calculate a reference voltage ( $V_{ref}$ ) which is used to produce the PWM control signal. The dc/dc converter is driven by a DSP-based controller for fast-response and the overall system stability is improved by including a PI controller which is also used to match the array and reference voltage levels. However, the DSP-based control unit increases the implementation cost of the system. Also, as explained in the description of the proposed system in Section IV, the measurement of the array voltage is not necessary for the power change detection, if the appropriate control software is used. A similar method has been proposed in [8], where the reference voltage is calculated as

$$V_{ref,k+1} = V_{ref,k} + M \cdot \frac{\Delta P_k}{\Delta V_k} \quad (3)$$

where

- $k, k + 1$  sampling instants;
- $M$  step size;
- $\Delta P_k / \Delta V_k$  instantaneous power slope at the solar array output.

The step size  $M$  is chosen according to the system stability requirements. Both previous methods have the disadvantage that

two control loops are required; the first to control  $V_{ref}$ , and the second to control the array voltage according to the reference voltage set in the first loop, so the control system design is complicated because of interaction between these loops.

Most of the preceding MPPT design methods are based on the regulation of the PV array output voltage or current according to a reference voltage or current signal, which is either constant or is derived from the PV array output characteristics (e.g., power or power change). A variation of these methods is to directly use the dc/dc converter duty cycle as a control parameter and force the derivative  $dP/dD$  to zero, where  $P$  is the PV array output power and  $D$  is the duty cycle, thus only one control loop is required. In [9] an analog controller is proposed, where a dc/dc converter is controlled so that  $dI_{out}/dD$  equals zero, where  $I_{out}$  is the dc/dc converter output current. However, this method cannot be applied when the converter operates in the discontinuous conduction mode, because in that case the duty cycle is a nonlinear function of the output current, and thus, local power maxima could exist and the MPPT cannot assure the overall maximum power output. In PV applications, the converter may operate in the discontinuous conduction mode in case of low irradiation, so the application of the above method results in power loss. Also, if the converter is designed to operate in the continuous conduction mode even for small input power levels, then a large output inductor is required which increases the system size and cost.

In the method proposed here [Fig. 7(a)], a microcontroller is used to measure the PV array output power and to change the

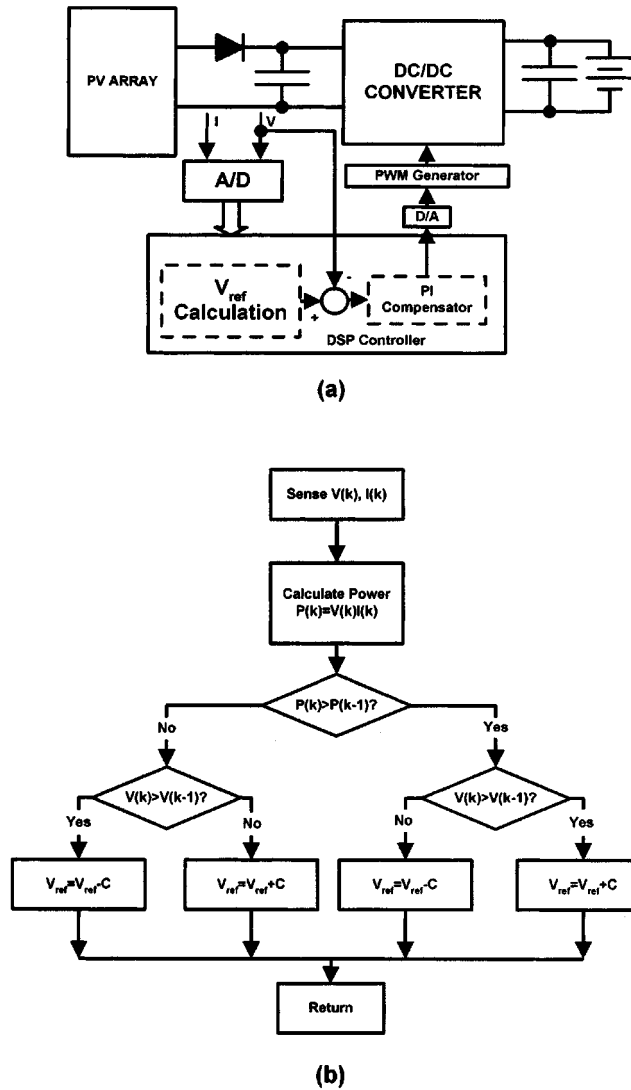


Fig. 2. DSP-controlled maximum power point tracking system: (a) the block diagram and (b) the MPPT control flowchart.

duty cycle of the dc/dc converter control signal. By measuring the array voltage and current, the PV array output power is calculated and compared to the previous PV array output power. Depending on the result of the comparison, the duty cycle is changed accordingly and the process is repeated until the maximum power point has been reached. The proposed system could be easily implemented also with analog circuits, instead of using a microcontroller, but the design described above has the advantage that it permits easy modification, if additional renewable energy sources (e.g., more PV arrays or wind generators) are used. Also, in case that the system is used in a solar-powered vehicle, the microcontroller MPPT algorithm can be easily modified to examine the existence of multiple local maxima in the array P-V curve, which might occur because of array damage or partial shading.

The implementation of the proposed method uses a low-cost, low-power consumption microcontroller, which controls a high-efficiency Buck-type dc/dc converter and performs all control functions required by the MPPT process and battery charging, if required.

This paper is organized as follows: the PV module and Buck converter characteristics are analyzed in Sections II and III, respectively, the proposed system design is presented in Section IV and the theoretical and experimental results are given in Section V.

## II. PV MODULE CHARACTERISTICS

The equivalent circuit of a PV module is shown in Fig. 3(a), while typical output characteristics are shown in Fig. 3(b). The characteristic equation for this PV model is given by [10], [11]

$$I = I_{LG} - I_{os} \left\{ \exp \left[ \frac{q}{AkT} (V + IR_s) \right] - 1 \right\} - \frac{V + IR_s}{R_{sh}} \quad (4)$$

where

$$I_{os} = I_{or} \left[ \frac{T}{T_r} \right]^3 \exp \left[ \frac{qE_{GO}}{Bk} \left( \frac{1}{T_r} - \frac{1}{T} \right) \right]$$

$$I_{LG} = [I_{SCR} + K_I(T - 25)]\lambda/100$$

and

|                                |   |
|--------------------------------|---|
| $I$ and $V$                    | cell output current and voltage;  |
| $I_{os}$                       | cell reverse saturation current;  |
| $T$                            | cell temperature in $^{\circ}\text{C}$ ;  |
| $k$                            | Boltzmann's constant;   |
| $q$                            | electronic charge;  |
| $K_I = 0.0017$                 | short circuit current temperature coefficient at $I_{SCR}$ ;                    |
| $A/^{\circ}\text{C}$           |   |
| $\lambda$                      | solar irradiation in $\text{W}/\text{m}^2$ ;                                    |
| $I_{SCR}$                      | short-circuit current at $25^{\circ}\text{C}$ and $1000 \text{ W}/\text{m}^2$ ; |
| $I_{LG}$                       | light-generated current;  |
| $E_{GO}$                       | band gap for silicon;   |
| $B = A = 1.92$                 | ideality factors;   |
| $T_r = 301.18^{\circ}\text{K}$ | reference temperature;  |
| $I_{or}$                       | cell saturation current at $T_r$ ;  |
| $R_{sh}$                       | shunt resistance;   |
| $R_s$                          | series resistance.  |

The variation of the output I-V characteristics of a commercial PV module as function of temperature and irradiation is shown in Fig. 4(a) and (b), respectively. It is seen that the temperature changes affect mainly the PV output voltage, while the irradiation changes affect mainly the PV output current. The intersection of the load-line with the PV module I-V characteristic, for a given temperature and irradiation, determines the operating point. The maximum power production is based on the load-line adjustment under varying atmospheric conditions.

## III. BUCK CONVERTER ANALYSIS

The Buck converter equivalent circuit diagram and its associated theoretical waveforms are shown in Figs. 5 and 6, respectively. Depending on the load and the circuit parameters, the inductor current can be either continuous [ $i_L(t) \geq 0$ ] or discontinuous [ $i_L(t) = 0$  before the end of the switching period].

The inductor value,  $L$ , required to operate the converter in the continuous conduction mode is calculated such that the peak

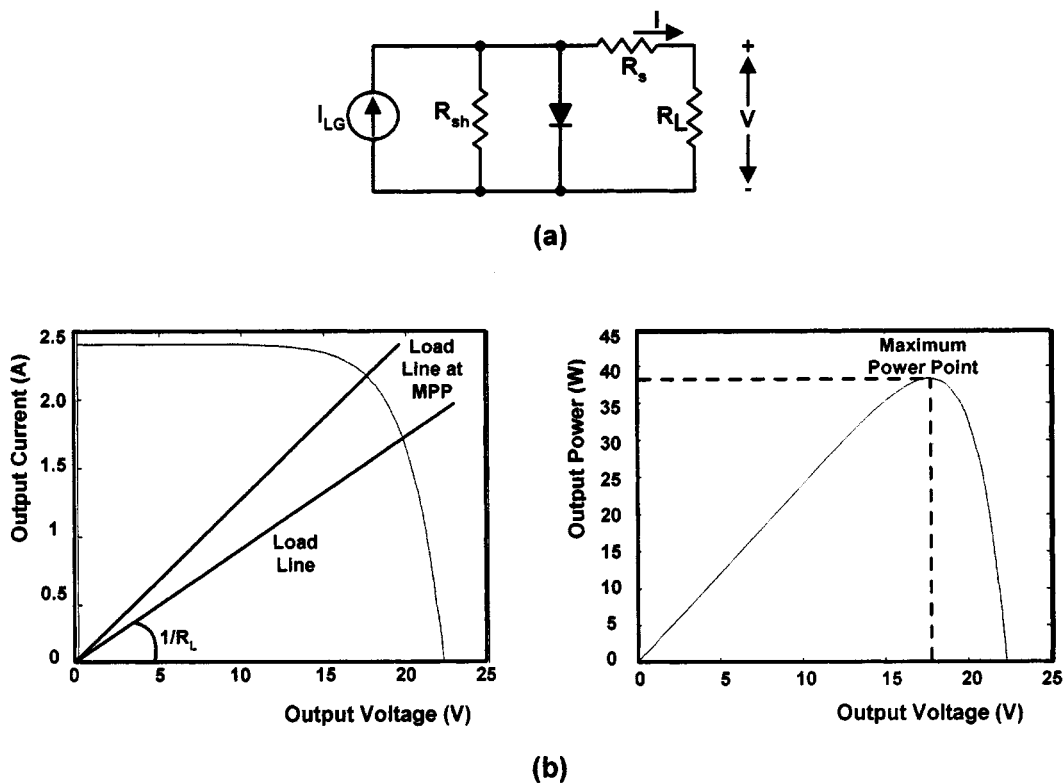


Fig. 3. (a) Equivalent circuit of a PV module and (b) typical PV module current-voltage and power-voltage characteristics.

inductor current at maximum output power does not exceed the power switch current rating [12]. Thus,  $L$  is calculated as

$$L \geq \frac{V_{om}(1 - D_{cm})}{f_s |\Delta I_{Lm}|} \quad (5)$$

where

|                 |           |   |
|-----------------|-----------|---|
| $f_s$           | $= 1/T_s$ | switching frequency;  |
| $D_{cm}$        |           | duty cycle at maximum converter output power;               |
| $\Delta I_{Lm}$ |           | peak-to-peak ripple of the inductor current;                |
| $V_{om}$        |           | maximum of the dc component of the output voltage;          |
| $I_{om}$        |           | dc component of the output current at maximum output power. |

The output capacitor value calculated to give the desired peak-to-peak output voltage ripple is

$$C \geq \frac{D_{cm} I_{om}}{r f_s V_{om}} \quad (6)$$

where  $r$  is the output voltage ripple factor defined as  $r = (\Delta V_{om}/V_{om})$  (usually  $r < 2\%$ ) and  $\Delta V_{om}$  is the output voltage peak-to-peak ripple at maximum power.

Taking into account that the ripple of the PV output current must be less than 2% of its mean value, [12], the input capacitor value is calculated to be

$$C_{in} \geq \frac{(1 - D_{cm}) I_{om} D_{cm}}{0.02 I_{pvm} R_{pvm} f_s} \quad (7)$$

where  $I_{pvm}$  is the converter input current at maximum input power, while  $R_{pvm}$  is the PV array internal resistance at the maximum power point and is defined as

$$R_{pvm} = \frac{V_{inm}}{I_{pvm}} \quad (8)$$

where  $V_{inm}$  is the PV array output voltage at the maximum power point.

When the Buck converter is used in PV applications, the input power, voltage and current change continuously with the atmospheric conditions, thus the converter conduction mode changes since it depends on them. Also, the duty cycle  $D_c$  is changed continuously in order to track the maximum power point of the PV array. The choice of the converter switching frequency and the inductor value is a compromise between converter efficiency, cost, power capability and weight. For example, the higher the switching frequency, the lower the inductor core size, but the power switch losses are higher. Also, by using a large  $L$  value, the peak-to-peak current ripple  $\Delta I_L$  is smaller, requiring lower current rating power switches, but the converter size is increased substantially because a larger inductor core is required.

#### IV. PROPOSED SYSTEM

A block diagram of the proposed system is shown in Fig. 7(a). A Buck-type dc/dc converter is used to interface the PV output to the battery and to track the maximum power point of the PV array. A more detailed diagram is illustrated in Fig. 7(b). The converter power switch consists of one or more parallel-connected power MOSFET's. The flyback diode  $D$  is of a fast switching type. The output inductor is wound on a ferrite-core with air-gap to prevent core saturation that might be caused by a large dc current component value. The inductor together with the input and output capacitor values are calculated according to the procedure described in the Appendix.

In the configuration of Fig. 7(b) a battery stack is used as the PV array load. For given atmospheric conditions, the bat-

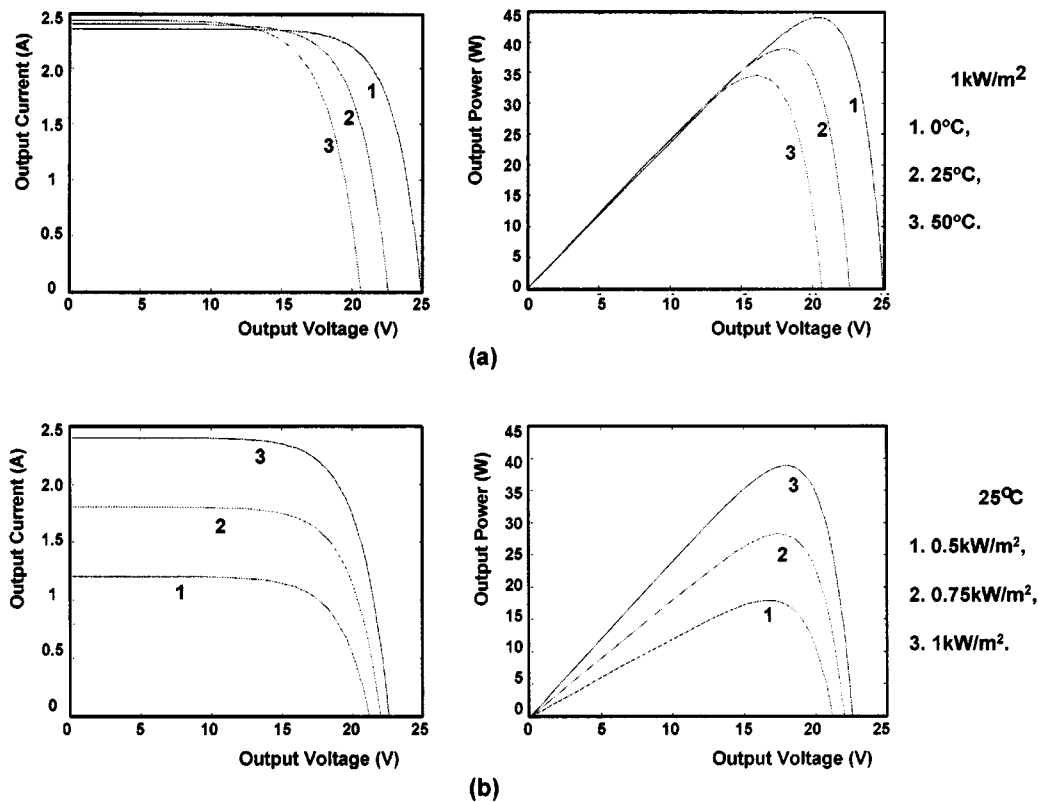


Fig. 4. Eharacteristic of a PV module with temperature and irradiation: (a) constant irradiation and varying temperature and (b) constant temperature and varying irradiation.

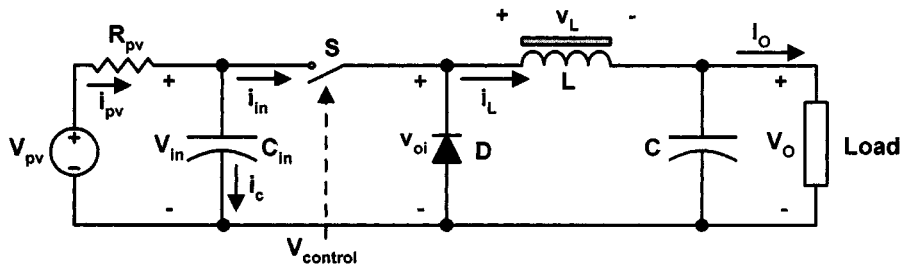


Fig. 5. Equivalent circuit diagram of the Buck converter.

ttery charging current depends on the PV output power and the battery voltage. The battery voltage increases according to the charging level and it is monitored to prevent overcharging.

The system control unit consists of:

- Intel's 80C196KC low-power consumption, CMOS microcontroller with external EPROM and SRAM;
- interface circuits which comprise of sensors and signal conditioners connected to the microcontroller A/D converter;
- IC driver for the power MOSFET(s).

The power consumed by the control unit is about 1 W and supplied by the battery which is being charged by the dc/dc converter.

The microcontroller unit 80C196KC features a 10-bit, eight-channel, successive approximation A/D converter, used by the control program to measure the signals required for the power flow control. The 10-bit resolution is adequate for the present application. Also, it features three PWM outputs with program-

controlled duty cycle and 39.2-kHz maximum frequency when driven by the 20-MHz clock of the unit. Each of the PWM outputs can be used to control a separate MPPT system. This type of microcontroller was chosen because it has the necessary features for the proposed system, such as an on-chip A/D converter, PWM outputs, 16-bit architecture, high clock rate, low-power consumption and low cost.

The converter input current,  $i_{in}$ , has the pulse-type waveform shown in Fig. 6(a) and (b) for both continuous and discontinuous conduction modes. A current transformer with a rectifier-RC filter combination can be connected to the secondary winding for the measurement of the current mean value which is proportional to the PV array output current. For a higher accuracy, a Hall-effect sensor or a current shunt could be used. However, the Hall-effect sensor is more expensive and the current shunt has more power losses.

The flowchart of the control program is shown in Fig. 8. "Slope" is a program variable with values either 1 or -1, indi-

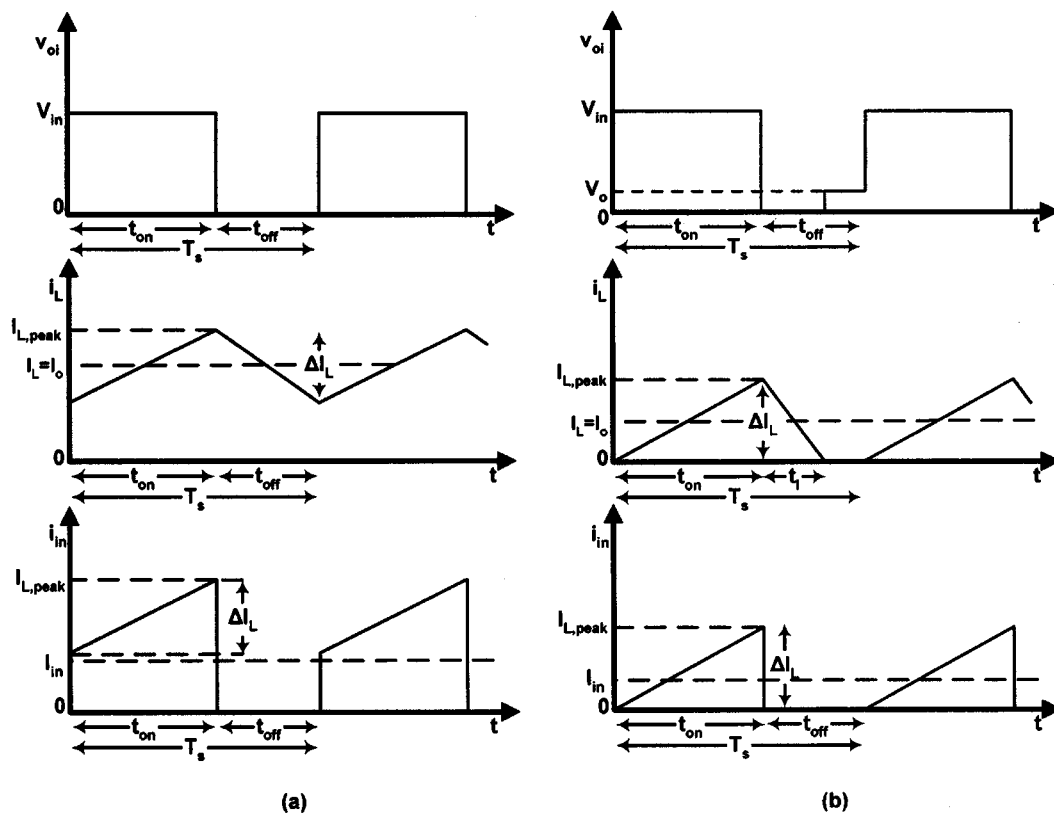


Fig. 6. Buck converter waveforms (a) continuous conduction mode and (b) discontinuous conduction mode.

ating the direction that must be followed on the hill-shaped PV array output power curve in order to increase its output power, while “ $\alpha$ ” is a constant between 0 and 1. Since an 8-bit CPU register is used to store the PWM duty cycle in the present application, the value of “ $\alpha$ ” is made equal to  $1/256$ . Initially, the value of “Slope” is set to 1. In each iteration, the dc/dc converter input voltage and current are measured and the input power is calculated. The input power is compared to its value calculated in the previous iteration and according to the result of the comparison, the sign of “Slope” is either complemented or remains unchanged. Then, the PWM output duty cycle is changed accordingly. The MPP tracking process is shown in Fig. 8(b). The starting points vary, depending on the atmospheric conditions, while the duty cycle is changed continuously, according to the above-mentioned algorithm, resulting in the system steady-state operation around the maximum power point. The battery voltage is monitored continuously and, when it reaches a pre-determined level, the battery charging operation is stopped in order to prevent overcharging.

## V. THEORETICAL AND EXPERIMENTAL RESULTS

A prototype MPPT system has been developed using the above-described method and tested in the laboratory. The PV array, which is to be used with this system, consists of 16 AEG, PQ10/40 type modules, giving a 614.4 W maximum power and an 89.6 V open-circuit voltage at an irradiation of  $1 \text{ kW/m}^2$  and a temperature of  $25^\circ\text{C}$ . The PV module specifications given by the manufacturer are shown in Fig. 9. In order to test the proposed system under various atmospheric conditions, the PV

array was first simulated with a dc power supply by adjusting its output voltage and current limit settings. The power switch consists of two MOSFET’s rated at 200 V, 30 A each, while the flyback diode has a 200 ns reverse-recovery time. The calculated input and output capacitor values are  $470 \mu\text{F}$  and  $4700 \mu\text{F}$ , respectively. The output inductor value is  $30 \mu\text{H}$  and is wound on a ferrite core with a 3-mm air gap.

The system efficiency is defined as

$$\eta = \frac{P_o}{P_{in}} = \frac{P_o}{P_o + P_d} \quad (9)$$

where  $P_{in}$  and  $P_o$  are the dc/dc converter input and output power, respectively, while  $P_d$  is the power loss. The power loss consists of the MOSFET and diode conduction and switching losses, the inductor core and copper losses and the control system power consumption.

The theoretical values were calculated using data given by the manufacturers of the circuit elements. The theoretical and measured efficiency for various output power levels is shown in Fig. 10. It is seen that the efficiency is quite high and relatively constant for a wide output power range.

The actual PV output power and the corresponding theoretical maximum output power for various irradiation levels is shown in Fig. 11(a). It is seen that the proposed system always tracks the PV maximum power point. Fig. 11(b) shows the PV output power for various irradiation levels, with the MPPT control disconnected and with the dc/dc converter duty cycle set such that the PV array produces the maximum power at  $1 \text{ kW/m}^2$  at  $25^\circ\text{C}$ . The theoretical maximum PV power at each irradiation level is also indicated in the figure. A comparison

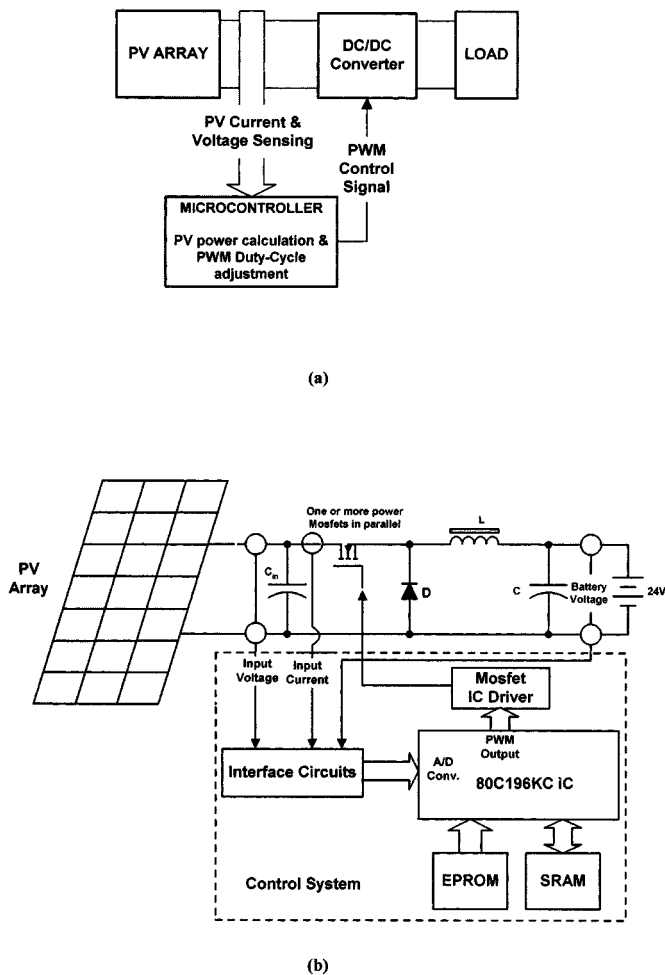


Fig. 7. Proposed system: (a) block diagram and (b) more detailed diagram.

between Fig. 11(a) and (b) shows that the use of the proposed MPPT control system increases the PV output power by as much as 15% for irradiation in the range of 0.2–0.75 kW/m<sup>2</sup> at 25 °C. As explained in Section IV, the MPPT operation in the proposed system is based on the dc/dc converter control algorithm using the actual PV array output power irrespective of the irradiation and temperature conditions, so the system performance for different operating atmospheric conditions was not further investigated.

The execution time of the control algorithm loop, shown in Fig. 8(a), has been calculated to be less than half a millisecond, while the time constant of the dc/dc converter is of the order of several milliseconds. Since both the sun irradiation and the air temperature change slowly during the daytime, the system is expected to track effectively the PV maximum power point, under normal changes of atmospheric conditions (e.g., cloud shadowing). This has been also verified experimentally by partially covering the PV modules and noting that the system tracked successfully.

The power MOSFET source voltage waveforms when the dc/dc converter operates in the continuous and the discontinuous conduction modes observed on an oscilloscope are shown in Fig. 12(a) and (b), respectively. The ringing observed in the discontinuous conduction mode is caused by the parasitic ca-

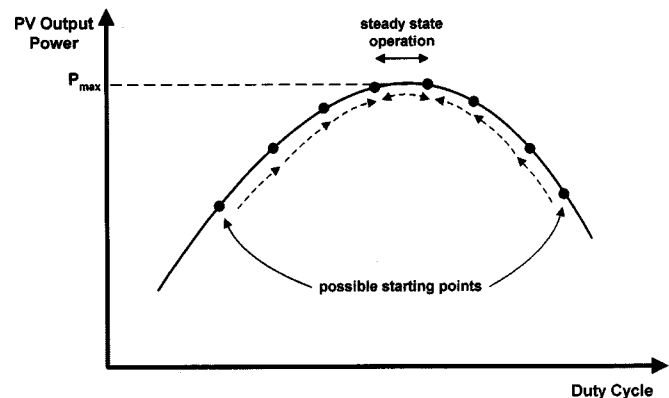
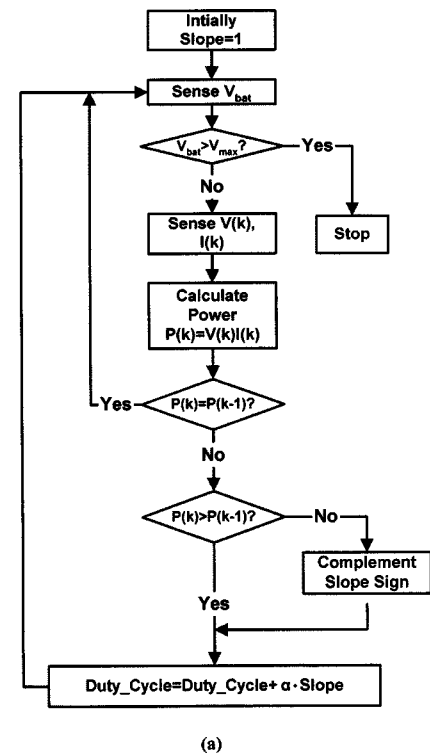


Fig. 8. MPPT control: (a) program flowchart and (b) MPP tracking process.

| Cell Temperature          | 0°C  | 25°C | 60°C |
|---------------------------|------|------|------|
| Open-circuit Voltage (V)  | 24.6 | 22.4 | 19.2 |
| Short-circuit Current (A) | 2.37 | 2.41 | 2.46 |
| Maximum Power Current (A) | 2.18 | 2.20 | 2.23 |
| Maximum Power (W)         | 42.6 | 38.4 | 32.4 |

Fig. 9. PV module specifications under standard test conditions (A.M. = 1.5 and irradiation = 1 kW/m<sup>2</sup>).

pacitance of the MOSFET source and the output inductor [13], but it does not affect the MPPT operation.

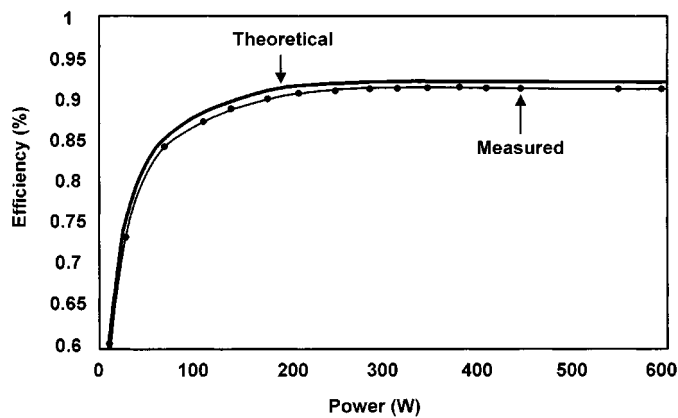
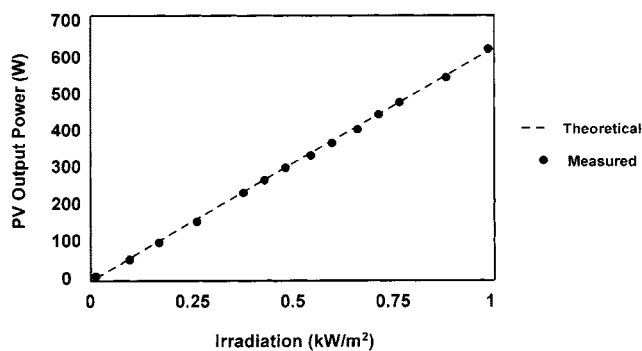
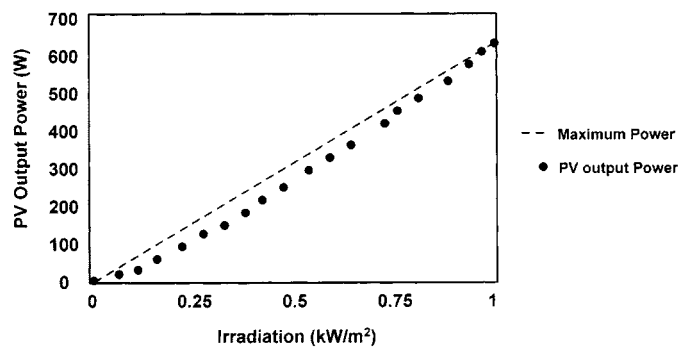


Fig. 10. System efficiency under PV MPPT conditions at 25 °C.



(a)



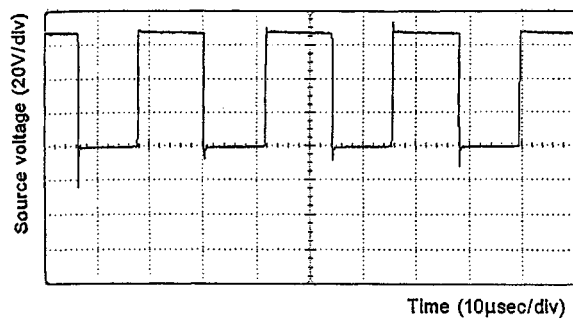
(b)

Fig. 11. (a) Theoretical and measured PV output power under MPPT conditions at various irradiation levels and (b) the actual PV output power and the corresponding theoretical maximum PV power at various irradiation levels when the dc/dc converter duty cycle is set such that the PV array produces the maximum power at 1 kW/m<sup>2</sup> at 25 °C.

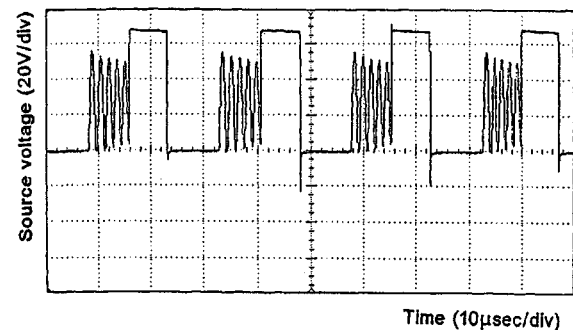
The measured input and output voltage ripple factors are 1.4% and 0.5%, respectively, under full-loading conditions.

## VI. CONCLUSION

The PV array output power delivered to a load can be maximized using MPPT control systems, which consist of a power conditioner to interface the PV output to the load, and a control unit, which drives the power conditioner such that it extracts



(a)



(b)

Fig. 12. Oscilloscope MOSFET source voltage waveforms when the dc/dc converter operates in (a) the continuous conduction mode and (b) the discontinuous conduction mode.

the maximum power from a PV array. In this paper, a low-cost, low-power consumption MPPT system for battery charging has been developed and tested. The system consists of a high-efficiency, Buck-type dc/dc converter and a microcontroller-based unit which controls the dc/dc converter directly from the PV array output power measurements. Experimental results show that the use of the proposed MPPT control increases the PV output power by as much as 15% compared to the case where the dc/dc converter duty cycle is set such that the PV array produces the maximum power at an irradiation level of 1 kW/m<sup>2</sup> and 25 °C.

The proposed control unit can be implemented also with analog circuits, but the microcontroller-based alternative was chosen since it permits easy system modifications. The proposed system can be used in a hybrid system where the microcontroller performs simultaneously the MPPT control of more than one renewable energy source. Furthermore, it can be coupled with an uninterruptible power supply system in commercial buildings or it can be used to supply power to the electrical grid through a dc/ac converter.

## ACKNOWLEDGMENT

The authors wish to thank E. Perdikakis for his assistance during the construction phase of the prototype and for laboratory measurements.



## REFERENCES

- [1] H. D. Maheshappa, J. Nagaraju, and M. V. Krishna Murthy, "An improved maximum power point tracker using a step-up converter with current locked loop," *Renewable Energy*, vol. 13, no. 2, pp. 195–201, 1998.
- [2] B. K. Bose, P. M. Szczesny, and R. L. Steigerwald, "Microcomputer control of a residential power conditioning system," *IEEE Trans. Ind. Applicat.*, vol. IA-21, pp. 1182–1191, Sept./Oct. 1985.
- [3] A. A. Nafeh, F. H. Fahmy, O. A. Mahgoub, and E. M. El-Zahab, "Developed algorithm of maximum power tracking for stand-alone photovoltaic system," *Energy Sources*, vol. 20, pp. 45–53, Jan. 1998.
- [4] K. Harada and G. Zhao, "Controlled power interface between solar cells and ac source," *IEEE Trans. Power Electron.*, vol. 8, pp. 654–662, Oct. 1993.
- [5] S. J. Chiang, K. T. Chang, and C. Y. Yen, "Residential energy storage system," *IEEE Trans. Ind. Electron.*, vol. 45, pp. 385–394, June 1998.
- [6] D. B. Snyman and J. H. R. Enslin, "Simplified feed-forward control of the maximum power point in PV installations," in *Proc. 1992 Int. Conf. Ind. Electron., Contr., Instrum. Automat.*, vol. 1, Nov. 1992, pp. 548–553.
- [7] C. Hua, J. Lin, and C. Shen, "Implementation of a DSP-controlled photovoltaic system with peak power tracking," *IEEE Trans. Ind. Electron.*, vol. 45, pp. 99–107, Feb. 1998.
- [8] P. Huynh and B. H. Cho, "Design and analysis of a microprocessor-controlled peak-power-tracking system," *IEEE Trans. Aerosp. Electron. Syst.*, vol. 32, pp. 182–189, Jan. 1996.
- [9] C. R. Sullivan and M. J. Powers, "A high-efficiency maximum power point tracker for photovoltaic arrays in a solar-powered race vehicle," in *Proc. IEEE Power Electron. Spec. Conf.*, June 1993, pp. 574–580.
- [10] G. Vachtsevanos and K. Kalaitzakis, "A hybrid photovoltaic simulator for utility interactive studies," *IEEE Trans. Energy Conv.*, vol. EC-2, pp. 227–231, June 1987.
- [11] M. G. Jaboori, M. M. Saied, and A. A. Hanafy, "A contribution to the simulation and design optimization of photovoltaic systems," *IEEE Trans. Energy Conv.*, vol. 6, pp. 401–406, Sept. 1991.
- [12] N. Mohan *et al.*, *Power Electronics-Converters, Applications and Design*. New York: Wiley, 1989.
- [13] A. I. Pressman, *Switching Power Supply Design*. New York: McGraw Hill, 1994.



**Eftichios Koutroulis** was born in Chania, Greece, in 1973. He received the B.S. and M.S. degrees in electronics and computer engineering from the Technical University of Crete, Chania, in 1996 and 1999, respectively, where he is currently pursuing the Ph.D. degree in renewable energy sources.

His main research interests include renewable energy sources and power electronics.



**Kostas Kalaitzakis** (M'54) received the degree in electrical and mechanical engineering from the Technical University of Athens, Greece, in 1977 and the Ph.D. degree from the School of Electrical Engineering, Democritus University of Thrace, Greece, in 1983.

He is an Associate Professor in the Technical University of Crete, Greece. He served as Adjunct Assistant Professor at the Georgia Institute of Technology, Atlanta. His current R&D areas are in renewable energy sources, energy saving in buildings, power electronics, sensors and measurement systems, smart cards applications, fuzzy, neural and genetic decision support and control systems, bioengineering, and local operating networks.



**Nicholas C. Voulgaris** received the B.E.E. degree from the City University of New York and the M.S.E.E. and Ph.D. degrees from Columbia University, New York.

He was Member of Technical Staff, Bell Telephone Laboratories, a Research Engineer with NASA Research Center, and taught electrical engineering courses at the City University of New York, Columbia University, National Technical University of Athens, Greece, Democritus University of Thrace, Greece, and Technical University of Crete, Greece, where he has been a Professor since 1991. His research interests include the development of electronic circuits for renewable energy systems, power converters, and high efficiency Class E amplifiers.